Performance of a Kromek multi-channel analyser for a silicon photomultiplier - scintillator gamma ray detector

Contact: chris.armstrong@stfc.ac.uk

J.K. Patel
Loughborough University,
LE11 3UE, United Kingdom

C. D. Armstrong, D. Neely
Central Laser Facility, STFC,
OX11 0QX, United Kingdom

1 Introduction

Previous work has identified two charge-sensitive preamplifiers (CSPs) to be useful in a silicon photomultiplier (SiPM) - scintillator system which uses the photonuclear activation of ^{27}Al to detect 15-30 MeV gamma rays from laser-plasma interactions [1, 2]. In order to identify such activations, the system must be able to resolve scintillation event energies. Energy calibration can be achieved using the 511 keV and 1274 keV photopeaks of a ^{22}Na source, if the responses of the silicon photomultiplier and multi-channel analyser used can be assumed to be linear for the required 50 keV-2 MeV range. The gain and pulse lengthening properties of charge-sensitive amplifiers allows the matching of the SiPM linear output range to the linear response region of a multi-channel analyser (MCA) [2]. Here, a Kromek K102 multi channel analyser is characterised with two amplifiers for dynamic range, using a 520 nm LED pulsed at 400ns on a KETEK 2x2 SiPM array, where the LED simulates bismuth germanate (BGO) scintillation emission which peaks at wavelength $\lambda = 480$ nm. It is concluded that SiPM-BGO detectors with larger crystals can be used effectively with a high gain CR-112 CSP, despite the saturation limit of the amplifier. A lower gain CR-113 CSP is preferable for spectroscopy with smaller crystal SiPM-BGO detectors with better light collection efficiency.

2 SiPM pulses: unamplified and charge amplified

25 μm microcell KETEK SiPMs have peak photo detection efficiency (PDE) of $\approx$ 40% at BGO peak emission at 480 nm, and 30-35% at the LED peak emission at 520 nm [4]. As shown in Fig. 1, the unamplified peak voltage response of the 2x2 array of 3 mm x 3 mm SiPMs is a power law with the fractional transmittance, for pulse amplitudes up to 1 V. The 2x2 array also has an increased output ceiling of $\approx$ 3.4 V compared with $\approx$ 1 V for a single SiPM cell [3]. Oscilloscope digitisation noise sets the lower detectable pulse height at $\approx$ 2 mV. When pulses are passed through the high gain CR-112 charge sensitive preamplifier (CSP), the plateau (or 'tail') shape at low irradiance persists, as seen in the red curve in Fig. 1, implying that the unamplified dark current noise contribution of the SiPM is closely co-incident with the oscilloscope noise.

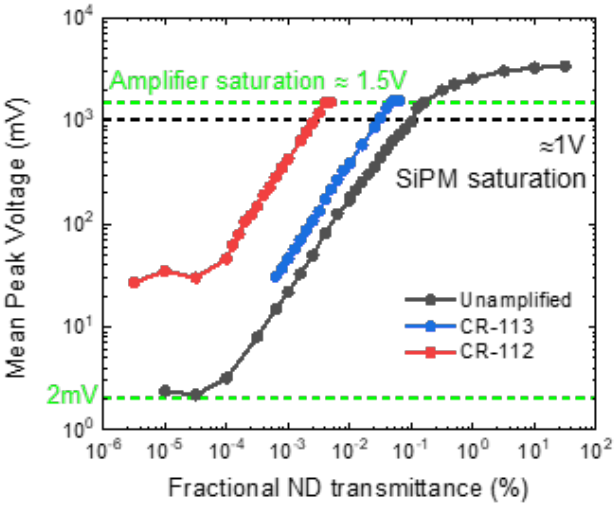

Figure 1: SiPM pulse heights, amplified with CR-112 and CR-113 and unamplified as a function of fractional transmission of LED light. Straight line regions indicate power law response with intensity for output pulse heights up to 1V. The gain of the two amplifiers brings different regions of the response into the dynamic range of the MCA

Cremat CSPs CR-112 and -113 have reported gains of (26.5$\pm$1.5)$\times$ and (2.6$\pm$0.8)$\times$, respectively [2]. However, the CSPs significantly change the pulses produced by the SiPM array beyond pulse height amplification, evident by comparing Figs. 5 and 6 in §5. Common to both the amplifiers is the inversion of the pulse polarity, pulse width increase, the introduction of zero-offsets, and a saturation limit of $\approx$ 1.5 V output pulse amplitude[1]. The increased pulse length offered by the charge amplifiers is a key benefit when using the MCA discussed in §3.

3 Kromek multi channel analyser with 2x2 SiPM pulses

Fig. 2 illustrates that Kromek MCA has a near linear response for 1-3 V unamplified pulse peak voltages. Below

[1]The trace offsets shown in Fig. 7 in §5 were corrected for before the plotting of the data in Fig. 1.

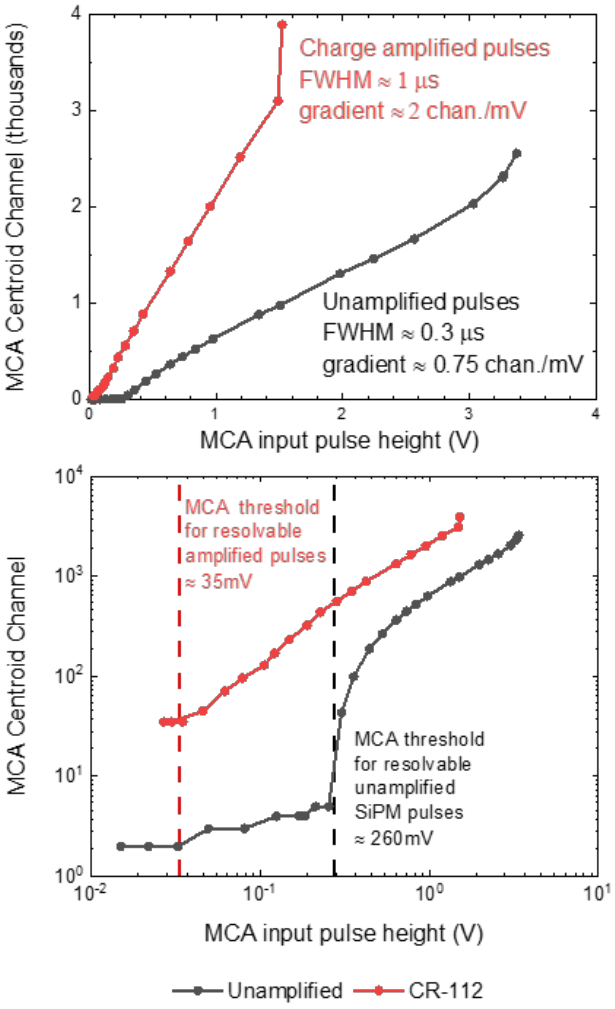

Figure 2: Centroid channels of MCA spectra vs. input pulse heights, with linear (top) and log-log (bottom) scaling. The MCA response is linear for unamplified input pulses of 1-3 V, and for longer pulse-width charge amplified pulses is linear for 0.1-1.5 V. Amplified response is shown for CR-112, but behaviour is identical with CR-113. MCA input measured with 50 Ω input impedance oscilloscope.

1 V, the response falls off rapidly, and pulses of <0.26 V cannot be resolved, registering outputs corresponding to just 2-3 channels (see lower plot, Fig. 8 in §5). Using CSPs reduces the lower resolution threshold of MCA input pulses down to 35 mV, and increases the gradient of the MCAs linear region to around 2 channels/mV. This is due to the amplifiers increasing the width of pulses from FWHM $\approx 0.27\ \mu s$ to $\approx 1.2\ \mu s$ (see Figs. 5 and 6), enabling easier digitisation of low amplitude pulses by the MCA.

Fig. 3 corrects the MCA input pulse heights for the gain of the respective amplifiers, to show the dynamic range of the MCA in terms of the amplitude of pulses

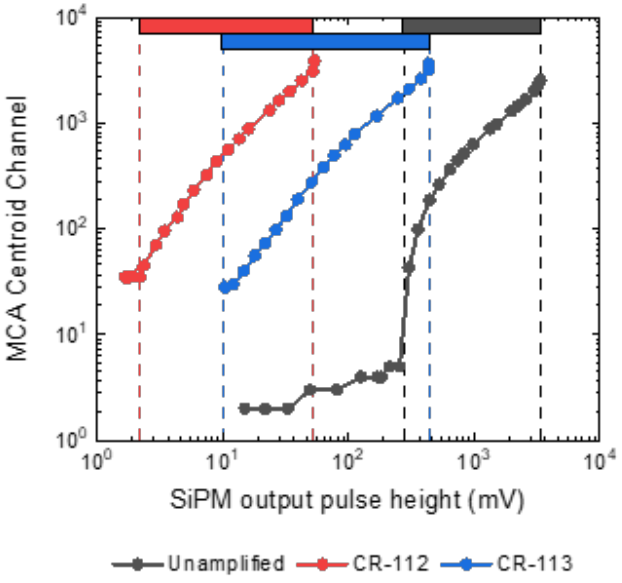

Figure 3: Centroid channels of MCA spectra vs. SiPM output pulse heights. Coloured rectangles and dashed lines indicate the respective dynamic range of the detector system with each amplifier, in terms of SiPM peak pulse voltage. SiPM pulse heights measured with impedance matched 50 Ω coupling, Kromek input impedance is 10 kΩ.

output by the SiPM. CR-112 is the higher gain amplifier ((26.5±2.5)×) and allows resolution of small optical pulses producing 2-50 mV amplitude electrical outputs from the SiPM. The lower gain ((2.8±0.8)×) CR-113 allows resolution of the 10-450 mV regime [2]. All measurements presented here were taken operating the SiPM at 30 V bias, which allows for the detection of the smallest pulses. However, operating at a lower bias voltage would bring higher energy scintillation events (larger amplitude optical pulses) below the saturation limits of the amplifiers, offering a route to further improved dynamic range [3, 4].

4 Conclusions

Using CSPs provides amplification and increased pulse widths, which increases the range of input pulse heights resolved by the Kromek MCA. The high gain provided by the CR-112 CSP enables rudimentary spectroscopy across the required 50 keV - 2 Mev range, given typical scintillation light collection efficiency of larger crystal detectors. Hence, the CR-112 is recommended where large volume detectors are required to suppress Compton scatter contributions, or in low activity environments. Reducing the bias voltage of silicon photomultipliers offers a route to increase the upper range of signals detectable below the saturation limit of the amplifier.

References

[1] R. J. Clarke et al. , 2006 *Detection of short lived radioisotopes as a fast diagnostic for intense laser-solid interactions*Appl. Phys. Lett. **89**, 141117 (2006)

[2] J.K. Patel *Gain characterisation of RF amplifiers for a silicon photomultiplier - scintillator gamma ray detector.* Central Laser Facility, (2019)

[3] A. Dasgupta *Application of Silicon Photomultipliers in Scintillation based radiation detectors.* Central Laser Facility, (2019)

[4] *Product Data Sheet: SiPM Silicon Photomultiplier, PM3325-WB-D0.* `https://www.ketek.net/wp-content/uploads/2018/12/KETEK-PM3325-WB-D0-Datasheet.pdf` KETEK GmbH., (2019)

[5] *SRS digital pulse generator datasheet* `https://www.thinksrs.com/downloads/pdfs/catalog/DG645c.pdf` Stanford Research Systems, (2019)

[6] *TENMA Bench Power Source datasheet* `http://www.farnell.com/datasheets/2724049.pdf?_ga=2.230339036.1795680448.1566202840-662613774.1566202840` TENMA, (2018)

[7] *PicoScope 6000 Series datasheet* `https://www.picotech.com/download/datasheets/PicoScope6000CDSeriesDataSheet.pdf` Pico Technology, (accessed 2019)

[8] *TENMA Bench Power Source datasheet* `http://www.farnell.com/datasheets/2724049.pdf?_ga=2.230339036.1795680448.1566202840-662613774.1566202840` TENMA, (2018)

[9] *Kromek K102 MCA datasheet* `https://info.kromek.com/k102-datasheet-download` Kromek Group plc., (accessed 2019)

[10] *Cremat CR-112 CSP specifications sheet* `https://www.cremat.com/CR-112-R2.1.pdf` Cremat Inc., (October 2018)

[11] *Cremat CR-113 CSP specifications sheet* `https://www.cremat.com/CR-113-R2.1.pdf` Cremat Inc., (October 2018)

5 Appendix

Equipment list

- SRS digital pulse generator. Part no.: DG645. [5]
- 520 nm LED
- Thorlabs absorptive neutral density filter set. Part no.: NEK01S
- KETEK SiPM chip: 2 x 2 array of 3 mm x 3 mm active area cells, containing 13,920 25 μm silicon avalanche photo-diode microcells. Part no.: PA3325-WB-D0-0202. [4]
- TENMA programmable bench DC power supply. Part no.: 72-2535. [6]
- PicoScope 6000 Series model: 6404D. [9]
- Kromek K102 Multi Channel Analyser. [8]
- Cremat CR-112 and -113 CSPs. [10], [11]
- Light shielding box.

Set up and procedure

1. The signal generator was powered up and the settings adjusted for a square wave output at 30 kHz and 400 ns pulse width, and connected directly to the PicoScope via a 10 dB signal attenuator. After recording the mean peak voltage of the pulses, the same signal was then connected to the Kromek, and a spectrum acquired. The channel number with the highest counts after $\approx$ 2 mins was recorded. This was repeated for pulsed through the interval 0.15 - 2.5 V.

2. The equipment was then set-up as shown in Fig. 4., with the pulse generator voltage now being fixed at 5 V, with the 10 dB attenuator removed. The 2x2 SiPM array was biased at 30 V with the TENMA DC power supply, but switched off at all times when the light shielding box was opened between measurements.

3. The irradiance on of the SiPM array was varied by using the Thorlabs ND filters to change the effective optical density from 0.5 - 7.0. The PicoScope was used to measure the mean peak voltage of the SiPM at each optical density, and then the Kromek MCA was used to record the spectral peak channel number.

4. Optical densities were converted to the fractional transmittance, and a linear fit carried out for the peak voltages in the region 3 mV - 1 V. The same was done plotting the MCA channel numbers against the peak voltages.

5. Steps 1-4 were repeated with subsequently added CR-112 and CR-113 amplifiers connected to the SiPM output, and the amplifier outputs connected to the PicoScope and/or the Kromek MCA.

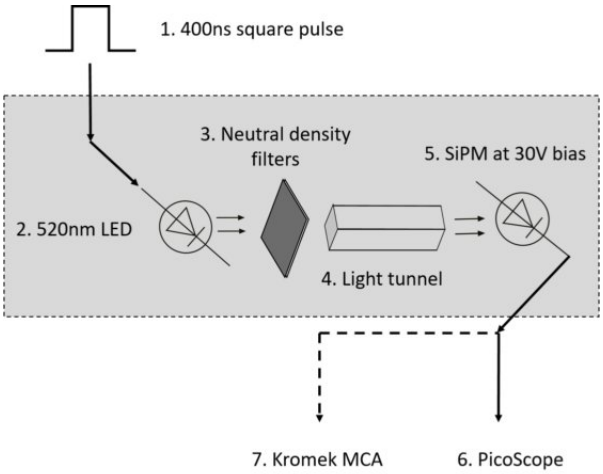

Figure 4: Block diagram of hardware set up. Shaded grey region indicates items in light shielding box.

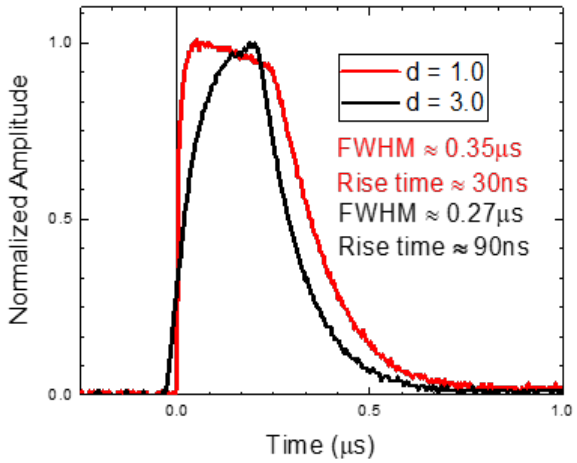

Figure 5: Example unamplified SiPM array output when exposed to 400 ns LED pulses. With the lower optical density ND filter, the SiPM is clearly saturated.

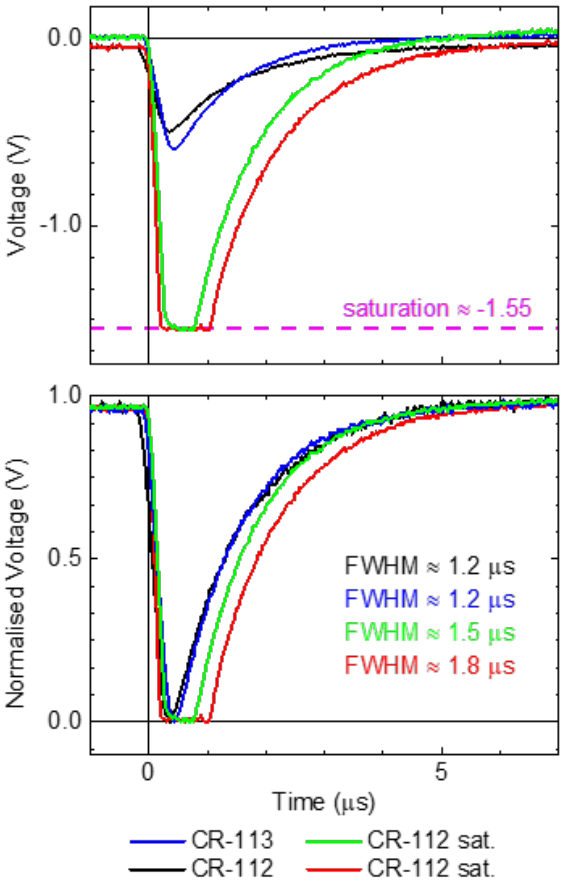

Figure 6: Example absolute (top) and normalised (bottom) charge amplified SiPM array pulse voltage profiles. Comparing with unamplified pulses in Fig. 5. shows effect of charge amplifiers on pulse shapes. Amplifier saturation has a more predictable effect on the pulse shape than saturation of the SiPM, with constant peak voltage and increasing pulse width, as shown with the FWHM values.

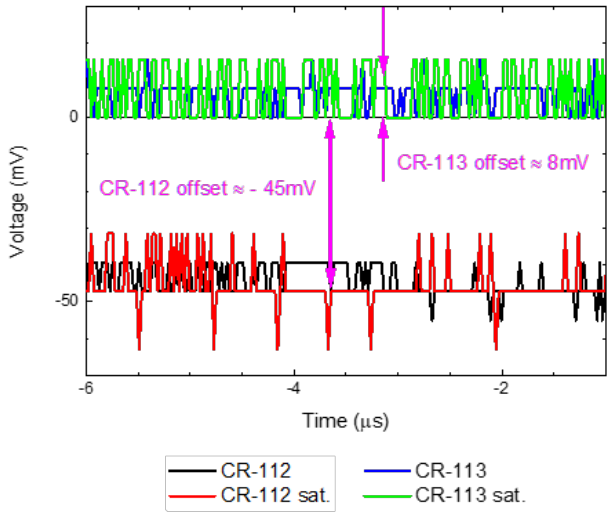

Figure 7: Pre-pulse zero-offsets of amplifier traces in Fig. 6.

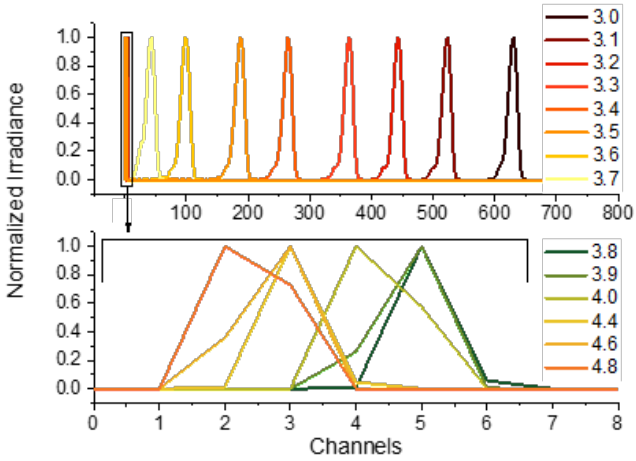

Figure 8: Kromek spectra for; top - resolvable pulses; bottom - unresolvable pulses. Legend indicates nominal optical densities used.

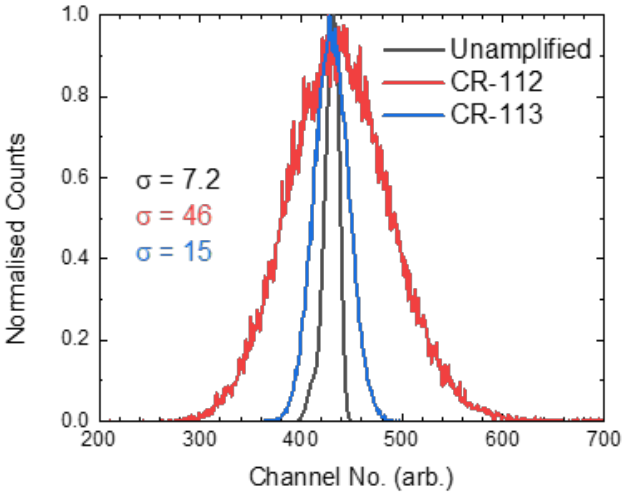

Figure 9: Kromek spectra for unamplified and charge amplified detector systems. Spectra shown have standard deviation values representative of the mean of the range of spectra obtained with different peak voltages.